Chapter 9

Thermal Degradation and Crystallisation Behaviour

The thermal degradation and crystallisation behaviour of PA12/PP blends are presented in this chapter. Effect of blend ratio and compatibiliser concentration on the thermal degradation properties of the blends are discussed in detail. The activation energy for degradation in compatibilised and uncompatibilised blends computed using Horowitz-Metzger equation is reported. Melting and crystallisation behaviours of the blends in the presence and absence of compatibilised are evaluated. The percentage crystallinity of neat polymers is measured and the variation of the percentage crystallinity as a function of blend ratio and compatibiliser concentration is presented.

The results of this chapter have been submitted for publication in ***Polymer Degradation and Stability***

9.1. Introduction

Thermal degradation and crystallisation behaviour of polymers and polymer blends are very relevant to the potential use of these materials in many demanding engineering applications. Thermal properties are important because of the fact that a study of stability of polymeric materials towards thermal degradation is one of the important criteria for designing these materials for engineering applications. Aliphatic polyamides (PAs) such as PA6, PA12, etc. are used in many demanding applications where the properties of thermal stability and fire resistance are priorities [1] and therefore have been extensively studied [2-5]. Polymer blending has been reported to have great impact on the thermal stability of polymers [6-17]. Compatibility between two components in a binary blend is one of the decisive factors, which determines the thermal stability of polymer blends [18-24], and therefore compatibilisation has profound effect on the thermal stability of polymer blends.

Crystallisation in polymer blends continues to attract a lot of interest because they involve important issues concerning control of super molecular structures as well as the corresponding physical and material properties. It has been reported that blending of polymers has significant impact on the crystallisation properties of individual polymer [7,21,25-55]. Although most of the research has focused on amorphous/crystalline polymer blends [25-46], few conclusive studies on crystalline/crystalline polymer blends exist [47-55].

Presence of compatibilisers may or may not affect the rate of crystallisation and spherulite morphology [21,23,51,55]. Moly et al. [55] have studied the thermal and crystallisation behaviour of linear low density polyethylene/poly (ethylene-co-vinyl acetate) (LLDPE/EVA) blends and found that the incorporation of EVA reduced the crystallinity of LLDPE phase in the blends. They also found that the crystallinity of the blends was not affected by compatibilisation.

The present chapter is centred on the investigation of the effect of blend ratio and addition of compatibilisers on the thermal and crystallisation behaviour of PA12/PP blends. Both PA12 and PP are semi-crystalline polymers. Fabrication and design of variety of articles with improved mechanical properties need a

detailed understanding of the thermal degradation of polymers because the threshold temperature for decomposition determines the upper limit of the fabrication temperature. At the same time, the changes in crystallisation behaviour of these polymers reflect in their end use properties. However the thermal and crystallisation behaviour of the component polymers in the blend are influenced by their relative amount, chemical compatibility and the level of dispersion achieved in the compounding process. Thermal stability and degradation kinetics were studied by thermo gravimetric (TGA) method. Differential scanning calorimetry (DSC) was used to determine the crystallisation behaviour of the blends.

9.2. Results and discussion

9.2.1. Thermal degradation properties

9.2.1.1. Individual polymer

The thermal decomposition of PA 12 can be explained on the basis of three mechanisms [56]: (a) free radical mechanism (b) cis elimination mechanism and (c) intermolecular exchange mechanism.

Free radical mechanism involves homolytic rupture, followed by disproportionation and dehydration as given below:

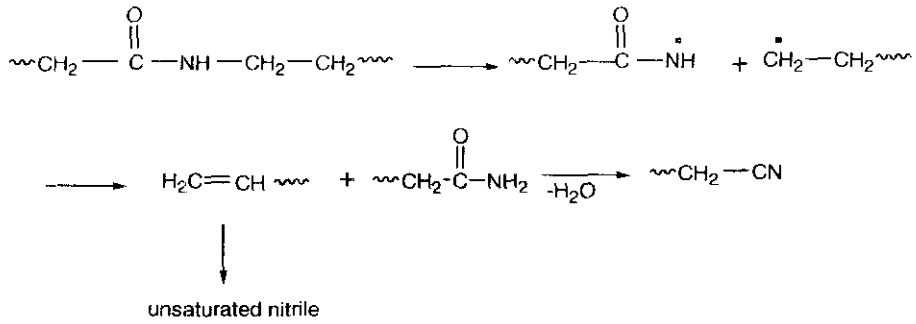

Cis elimination mechanism also leads to similar products as follows:

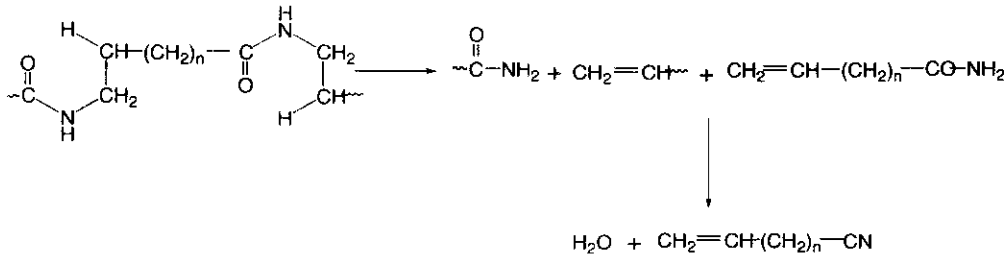

The third mechanism involves the intermolecular exchange and finally leads to a lactam.

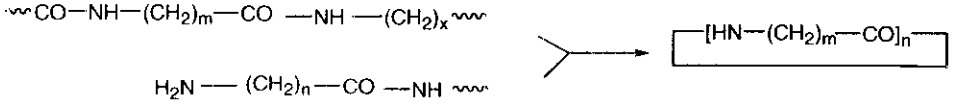

The thermal decomposition of PP involves the random chain scission and intermolecular transfer involving tertiary hydrogen abstractions from the polymer by the primary radical. The degradation products of PP involves monomer, 2-methyl 1-pentane, 2,4-dimethyl 1-heptane, 2-pentene and isobutene [57]. The mechanism of thermal decomposition of PP can be represented as follows:

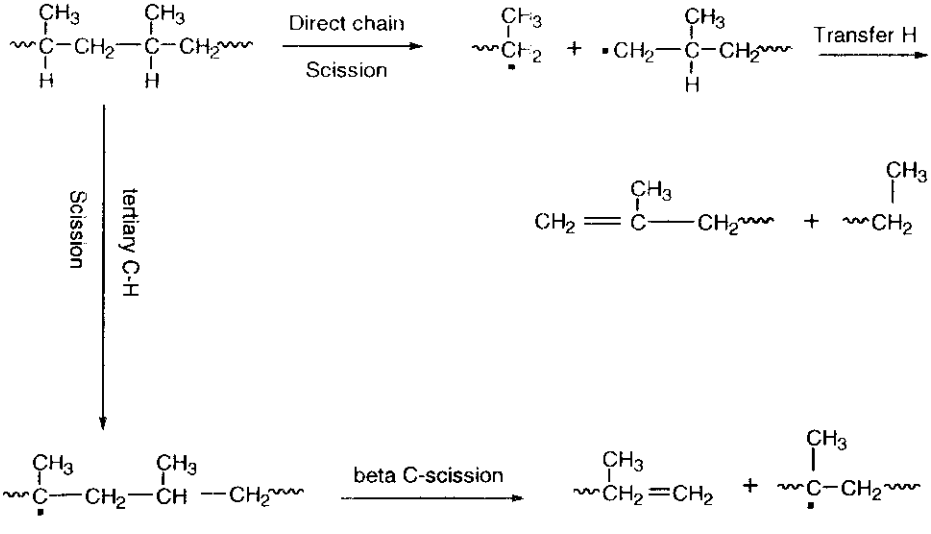

9.2.1.2. Uncompatibilised blends

Figures 9.1 and 9.2 present the thermograms (TGA) of PA12, PP and their blends whereas Figs. 9.3 and 9.4 give their derivative thermograms (DTG). The important results obtained from the figures are summarised in Tables 9.1-9.3.

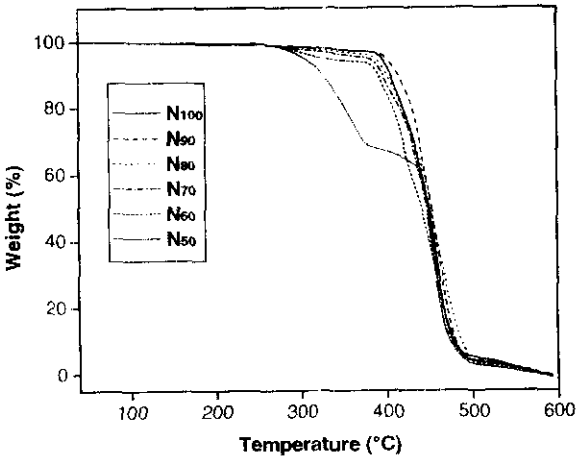

Figure 9.1: Effect of blend ratio on the thermograms of PA12/PP blends (PA12 is the major phase)

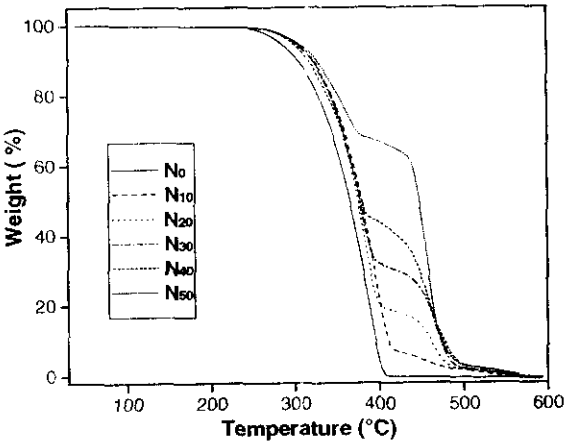

Figure 9.2: Effect of blend ratio on the thermograms of PA12/PP blends (PP is the major phase)

It is seen from the DTG curves (Figs. 9.3 and 9.4) that except N_{100}, N_{90}, N_{10} and N_0, all the other blends exhibit two degradation peaks corresponding to the degradation of PA12 and PP phases indicating the highly immiscible two-phase

structure of the blends. This doesn't mean that N_{90} and N_{10} are miscible systems. The morphology studies showed that these are phase separated blends (see Chapter 7). The occurrence of only one degradation temperature is due to two facts: (i) the concentration of dispersed phase is too small to possess a separate degradation peak and (ii) the sensitivity of TGA is not very high to resolve the degradation steps of individual polymer in multiphase polymer systems when its concentration is very low.

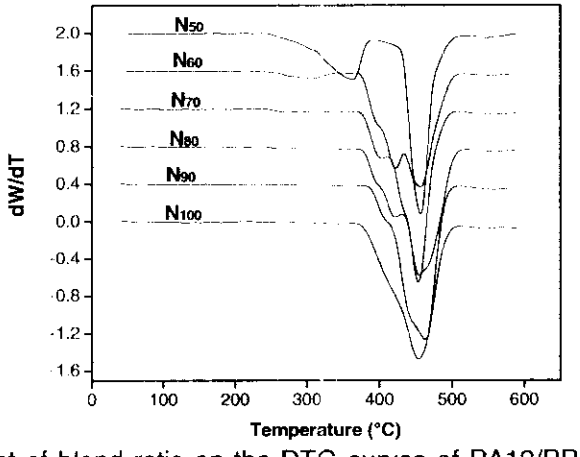

Figure 9.3: Effect of blend ratio on the DTG curves of PA12/PP blends (PA12 is the major phase)

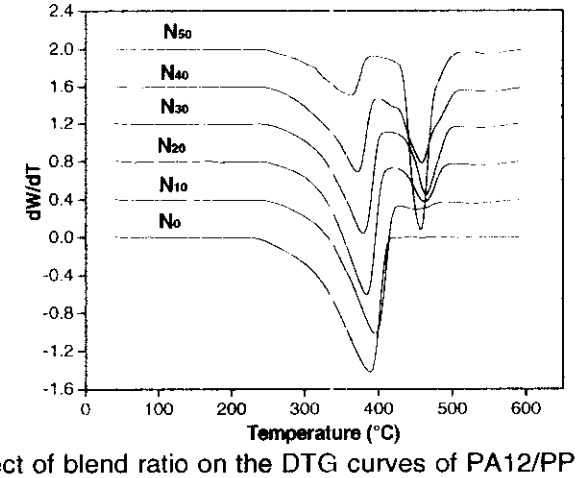

Figure 9.4: Effect of blend ratio on the DTG curves of PA12/PP blends (PP is the major phase)

Table 9.1 shows that addition of PP into PA12 decreases the thermal stability of the blends only marginally. 30wt% addition of PP into PA12 (N_{70}) decreases the T_{on} by 12°C. On the other hand, 50wt% addition of PP shows a remarkable decrease in T_{on}. It registered a decrease of more than 80°C. In addition, when we look at T_{10}, T_{20}, etc., it is seen that there is no considerable difference between N_{100} (neat PA12) and N_{70}. This is a clear evidence of the dependence of thermal stability on the phase morphology of the blends. It should be noted that N_{70} blends possess a matrix-droplet morphology in which thermally more stable PA12 forms the matrix whereas less stable PP forms the dispersed phase. In this case, the presence of 30wt% of the dispersed phase has no considerable deteriorating effect on the thermal stability of the blends since the matrix phase suppresses the degradation of dispersed phase. However, from the morphology studies, it is seen that N_{50} possesses a co-continuous phase structure in which both PA12 and PP form continuous phases (see Chapter 7). This situation makes PP phase to undergo degradation in a much faster rate.

Blends	T_{on}(°C)	T_{10}(°C)	T_{20}(°C)	T_{30}(°C)	T_{40}(°C)	T_{50}(°C)
N_{100}	394	405	420	433	442	450
N_{70}	382	397	416	430	439	447
N_{50}	310	327	352	373	442	448
N_{30}	290	322	344	358	368	377
N_0	270	304	329	345	356	366

Table 9.1: Effect of blend ratio on the temperatures corresponding to different percentage weight losses in PA12/PP blends

	Weight remained at temperature (%)			
Blends	**400(°C)**	**420(°C)**	**440(°C)**	**460(°C)**
N_{100}	93.1	80.1	61.8	32.4
N_{70}	88.4	77.8	58.8	26.7
N_{50}	66.87	64.85	38.8	24.2
N_{30}	32.7	30.1	27.4	19.2
N_0	3.8	0	0	0

Table 9.2: Effect of blend ratio on the weight remained at selected temperatures in uncompatibilised PA12/PP blends

In the case of T_{10}, T_{20}, etc., a remarkable difference is seen between N_{100} and N_{50}. The same situation exists in N_{30} blends. Note that in N_{30} blends, thermally less stable PP forms the matrix and therefore it is more prone to thermal degradation. However, compared to N_0 (PP), N_{30} is thermally more stable. T_{on} increases by ca. 20°C, T_{10} by ~18°C and T_{20} by ~15°C by the addition of 30wt% PA12 into PP. Thus one can claim that even though PP forms the matrix in N_{30} blends, it is thermally more stable compared to neat PP. This means that despite, PP and PA12 are immiscible and incompatible, the presence of PA in PP improves the thermal stability of the blends. Further, Table 9.2, which shows the effect of blend ratio on the percentage weight remained at different temperatures, gives a clear idea about the deterioration of thermal stability of PA12/PP blends with the addition of PP. Thus, it can be concluded that phase morphology plays a crucial role in determining the thermal stability of multiphase polymer systems.

Table 9.3 displays the effect of blend ratio on the T_{max} and IPDT of the blends. T_{max} is the temperature corresponds to maximum rate of degradation and IPDT is the integral procedural decomposition temperature (see chapter 5). It is seen that T_{max} and IPDT of PA12 is maximum (463 and 443°C, respectively) whereas those of PP are minimum (391 and 356°C, respectively) indicating that PA12 is y more thermally more stable than PP. All the blends exhibit two T_{max} values corresponding to the degradation of PA and PP phases. A gradual decrease in IPDT with the addition of PP into PA12 is observed. Note that there is no considerable difference between the IPDT of N_{100} (neat PA12) and N_{70} blends. On the other hand, the IPDT of N_{30} is appreciably greater than that of N_0 (neat PP). In summary, the thermal degradation studies of uncompatibilised PA12/PP blends revealed that the type of morphology has profound effect on the thermal stability of the blends. Thermal stability of the blends is not significantly affected by the addition of 30wt% of PP into PA12 since PA12 (which is thermally more stable) forms the matrix phase. On the other hand, when PP forms the matrix (in N_{30} blends), the thermal stability of the blends decreased drastically. Despite PP is the matrix phase, addition of 30wt% PA12 into PP resulted in improved thermal stability.

Blends	IPDT (°C)	T_{max}(°C)
N_{100}	443	463
N_{70}	438	453
N_{50}	416	459
N_{30}	389	380
N_0	356	391

Table 9.3: Effect of blend ratio on the T_{max} and IPDT of uncompatibilised PA12/PP blends

9.2.1.3. Compatibilised blends

Figures 9.5 and 9.6 present the effect of compatibilisation on the TG and DTG thermograms of N_{70} blends. It is evident from the DTG curves that compatibiliser has definite impact on the thermal degradation properties of the blends. Note that N_{70} possesses two degradation peaks corresponding to the degradation of PA12 and PP phases. But the peaks merge together with addition of compatibiliser. This implies the better interfacial adhesion due to the interface strengthening in the presence of compatibiliser.

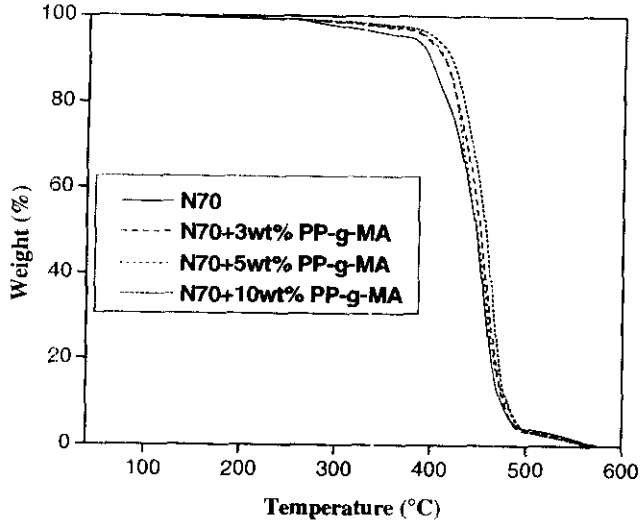

Figure 9.5: Effect of compatibilisation on the thermograms of N_{70} blends

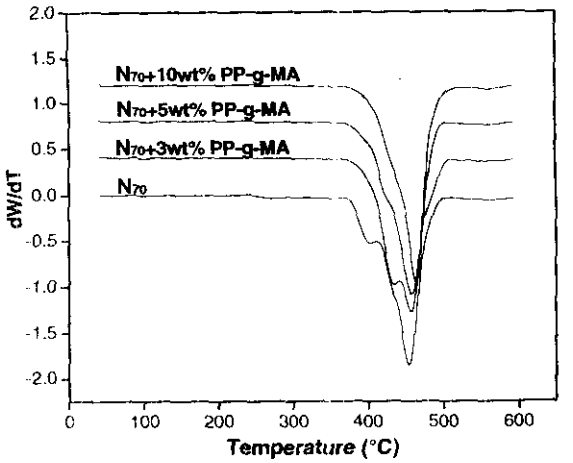

Figure 9.6: Effect of compatibilisation on the derivative thermograms of N_{70} blends

Blends	T_{on}(°C)	T_{10}(°C)	T_{20}(°C)	T_{30}(°C)	T_{40}(°C)	T_{50}(°C)
N_{70}	382	397	416	430	439	447
3% PP-g-MA	388	410	423	432	440	447
5% PP-g-MA	390	413	426	433	440	448
10% PP-g-MA	395	420	433	443	451	457

Table 9.4: Effect of compatibilisation on the temperatures corresponding to different percentage weight losses in N_{70} blends

Blends	Weight remained at temperature (%)			
	400(°C)	420(°C)	440(°C)	460(°C)
N_{70}	88.4	77.8	58.8	26.7
3% PP-g-MA	93.6	83	59.6	27.9
5% PP-g-MA	94.1	85.7	59.9	30.8
10% PP-g-MA	95.5	89.9	63.3	45

Table 9.5: Effect of compatibilisation on the weight losses at selected temperatures in N_{70} blends

Tables 9.4 and 9.5 demonstrate that there is remarkable improvement in thermal stability in the presence of compatibiliser. Note that the T_{on} increased by 13°C with the addition of 10wt% compatibiliser whereas there is remarkable reduction in the percentage weight loss at different temperatures. In addition, the IPDT and T_{max}

increased with increase in the addition of the compatibiliser. IPDT and T_{max} registered an increase of more than 10°C (Table 9.6).

Blends	IPDT (°C)	T_{max}(°C)
N_{70}	438	453
3wt% PP-g-MA	444	455
5wt% PP-g-MA	445	458
10wt% PP-g-MA	451	464

Table 9.6: Effect of compatibilisation on the T_{max} and IPDT of N_{70} blends

Figures 9.7 (TGA) and 9.8 (DTG) demonstrate the effect of compatibiliser on the thermal stability of N_{50} blends. From the thermograms it can be seen that blends underwent two-step degradation processes corresponding to the degradation of PA and PP phases. However, it is very important to note that both the thermograms, especially DTG thermograms, revealed that with the addition of compatibiliser the compatibility between the components in the blends increased. The DTG thermograms clearly demonstrate that with increase in compatibiliser concentration, the degradation peaks corresponding to PA and PP phases approach each other as in the case of N_{70} blends. Interestingly, the peak corresponds to PA splits into two peaks at higher compatibiliser concentrations.

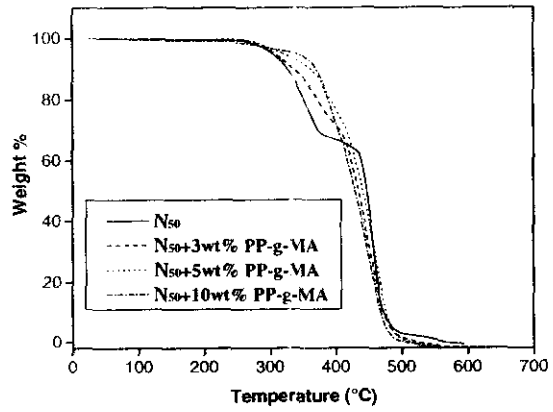

Figure 9.7: Effect of compatibilisation on the thermograms of N_{50} blends

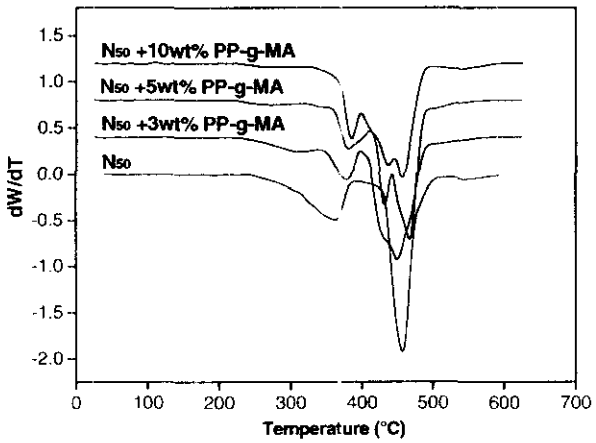

Figure 9.8: Effect of compatibilisation on the derivative thermograms of N_{50} blends

Blends	T_{on}(°C)	T_{10}(°C)	T_{20}(°C)	T_{30}(°C)	T_{40}(°C)	T_{50}(°C)
N_{50}	310	327	352	373	442	448
3wt% PP-g-MA	316	334	371	409	423	433
5wt% PP-g-MA	348	362	393	418	430	443
10wt% PP-g-MA	359	471	489	404	420	428

Table 9.7: Effect of compatibilisation on the temperatures corresponding to different percentage weight losses in N_{50} blends

Blends	IPDT (°C)	T_{max}(°C)		
N_{50}	416	360	---	459
3wt% PP-g-MA	418	380	---	450
5wt% PP-g-MA	428	380	432	468
10wt% PP-g-MA	420	384	436	459

Table 9.8: Effect of compatibilisation on the T_{max} and IPDT of N_{50} blends

From Table 9.7, it is clear that the T_{on} enhanced considerably in the presence of compatibiliser. With the addition 5wt% compatibiliser, T_{on} increased by ~ 40°C. In the other cases also, especially, for T_{10}, T_{20} and T_{30}, it is seen that thermal stability of the blends enhanced remarkably with the addition of 5wt% compatibiliser. Further, it can be seen from Table 9.8 that IPDT increased by ~12°C with the addition of 5wt% compatibiliser and beyond that level IPDT decreased. It should be noted that even in the presence of compatibiliser, the blends show two T_{max}

corresponding to PA and PP phases but the peaks approach each other in the presence of compatibiliser.

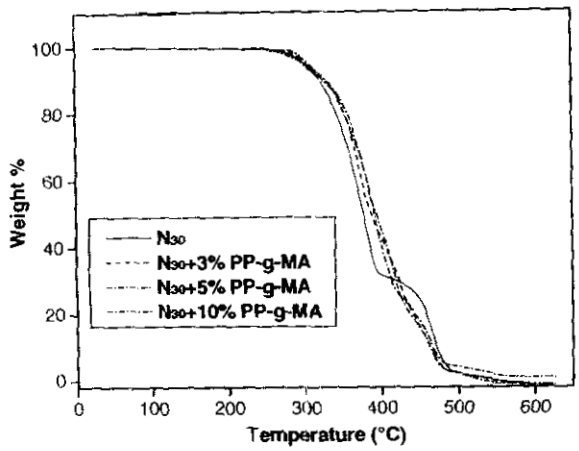

Figure 9.9: Effect of compatibilisation on the thermograms of N_{30} blends

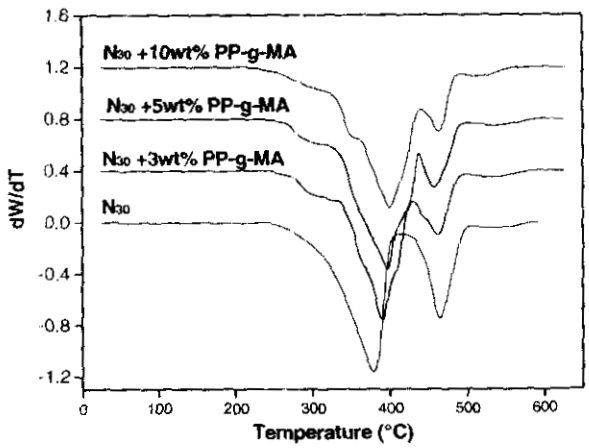

Figure 9.10: Effect of compatibilisation on the derivative thermograms of N_{30} blends

Blends	T_{on}(°C)	T_{10}(°C)	T_{20}(°C)	T_{30}(°C)	T_{40}(°C)	T_{50}(°C)
N_{30}	290	322	344	358	368	377
3wt% PP-g-MA	299	326	354	366	375	385
5wt% PP-g-MA	297	328	355	370	381	393
10wt% PP-g-MA	299	327	354	368	382	394

Table 9.9: Effect of compatibilisation on the temperatures corresponding to different percentage weight losses in N_{30} blends

Blends	IPDT (°C)	T_{max}(°C)	
N_{30}	389	379	465
3wt% PP-g-MA	392	396	458
5wt% PP-g-MA	395	389	462
10wt% PP-g-MA	393	399	463

Table 9.10: Effect of compatibilisation on the T_{max} and IPDT ofN_{30} blends

A similar conclusion can be derived from the thermograms of compatibilised N_{30} blends (Figs. 9.9 and 9.10). However, a relatively less rate of improvement in thermal stability is observed. T_{on} (Table 9.9) registered an increase of ~10°C with the addition of 3wt% compatibiliser. Further addition has little effect on T_{on}. The increase in IPDT with compatibiliser loading is not significant when compared to N_{50} and N_{70} blends. (Table 9. 10). In addition, even though the two peaks approach each other at higher compatibiliser concentration, no merging of peaks takes place.

In short, compatibilisation improved the thermal stability of the bends considerably. However, the rate of increase of thermal stability in various blends is in the order N_{70}>N_{50}>N_{30}. This is basically due to the fact that thermal stability of the blends mainly depends on the morphology of the blends; i.e., the type of morphology. The thermal stability of the immiscible polymer system mainly depends on the polymer which forms the matrix. If the thermally more stable polymer forms the matrix (in this case PA12), the thermal stability of the system is expected to be higher since the matrix phase protects the dispersed component from thermal degradation as seen in the case of N_{70} blends (note that the degradation peaks merged together in the presence of compatibiliser). However, the extent of improvement depends on the compatibility between the two polymers. On the other hand, if the thermally unstable system forms the matrix (in this case PP), even if the dispersed phase exhibits very high thermal stability, the thermal stability of the blends will be less than expected since the matrix phase is more prone to thermal degradation. In this case, the compatibilisation cannot provide considerable improvement in the thermal stability as seen in the case of N_{30} blends (see the compatibilised blends show two degradation peaks correspond to that of individual polymer). However, if the blends possess co-continuous phase structure, an intermediate behaviour is

seen as observed in the case of N_{50} blends (In this case, with the addition of compatibiliser, the peaks tend to approach each other, but at compatibiliser concentration, one of the peaks splits). Thus it can be concluded that the thermal stability of multiphase polymer systems depends on the type of morphology and the extent of compatibility between the individual components.

9.2.1.4. Activation energy

Horowitz Metzger equation was used for calculating the activation energy (E_a) of component polymers. The details of the equation are given in Chapter 5. Figure 9.11 shows the Arrhenius plots for calculating the E_a for degradation of PA12, PP and their blends. Table 9.11 gives the effect of blend ratio on the E_a of PA12//PP blends. The E_a of PA12 was found to be ~192kJ/mol and addition of 30wt% PP does not alter the E_a of PA12. This means that the thermal stability of the blends is not adversely affected by the addition of PP. Even though the DTG curve of N_{70} shows two degradation peaks we selected the degradation peak of PA12 as that of the blends since PA12 acts as the matrix. Similarly, in the case of N_{30} blends, we calculated E_a of the blends from degradation peak of PP since PP forms the major phase. On the other hand, for N_{50} blends, we presented E_a of the blends as the sum of the E_a of PA12 and PP since both form the continuous phase. E_a of PP was found to be ~124kJ/mol. It is important to note that the E_a of N_{30} blends is considerably higher than that of PP. This indicates that addition of PA12 enhanced the thermal stability of PP. The average E_a of N_{50} is found to be ~175kJ/mol. This is considerably greater than the E_a of PP and less than that of PA12. Note that E_a of N_{50} is even greater than the average of E_a of PA12 and PP (~158kJ/mol).

Regarding the effect of compatibilisation on the E_a of PA12/PP blends, we present compatibilised N_{70} as a representative. Table 9.12 gives the effect of compatibilisation on the E_a of N_{70} blends. It is important to note that E_a of the blends increased with compatibiliser addition. With 5wt% addition of compatibiliser, E_a increased by ~17% indicating considerable improvement in the thermal stability of the blends in the presence of compatibiliser. However, further addition of compatibiliser only marginally improved the thermal stability. This result is

in agreement with the morphology of the blends where 5wt% compatibiliser was found to be the CMC (see Chapter 7).

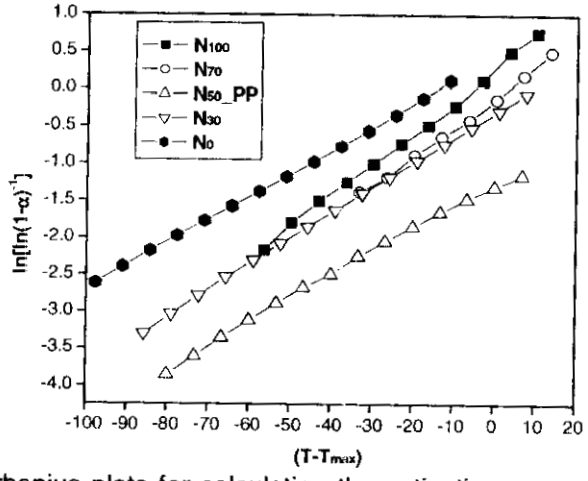

Figure 9.11: Arrhenius plots for calculating the activation energy for degradation of PA12, PP and their blends

Blends	E_a (kJ/mol)
N_{100}	192.1
N_{70}	192.8
*N_{50}	175
N_{30}	138.1
N_0	124.3

* the average value if taken as 175 (104+246)

Table 9.11: Activation energy of PA12, PP and their blends

Blends	E_a (kJ/mol)
N_{70}	192.8
3wt% PP-g-MA	207.2
5wt% PP-g-MA	225.1
10wt% PP-g-MA	227.5

Table 9.12: Effect of compatibilisation on the activation energy of N_{70} blends

9.2.2. Melting and crystallisation behaviour

9.2.2.1. Uncompatibilised blends

Figures 9.12 and 9. 13 present the DSC cooling and heating curves, respectively of PA12 and PP. (Note that the Y- axis of all the heating and cooling curves given in chapter is arbitrarily taken). The effect of blend ratio on the melting and crystallisation behaviour of uncompatibilised PA12/PP blends can be evaluated from the DSC cooling and heating curves of uncompatibilised blends given in Figs. 9.14 and 9.15, respectively. The melting and crystallisation parameters of PA12, PP and the effects of blend ratio on these properties are depicted in Tables 9.13 and 9.14. Table 9.13 gives the crystallisation (T_c) and melting (T_m) temperatures of PA12 and PP in virgin state and in the blends. The T_c of PA12 and PP is found to be 154 and 117°C, respectively while the T_m of PA12 and PP is 182 and 165°C, respectively. It is seen that blending has no effect on the T_c and T_m of the individual polymer. Similarly, table 9.14 shows that the normalised values of enthalpies of crystallisation (ΔH_c) and fusion (ΔH_f) are unaffected by blending. The percentage crystallinity of PA12 and PP was calculated using the equation:

$$\%crystallinity = \left(\Delta H_f / \Delta H_f^0\right) 100 \qquad (9.1)$$

where ΔH_f is the normalised enthalpy of fusion obtained calorimetrically and ΔH_f^0 is the enthalpy of fusion of the 100% crystalline PA12 and PP. ΔH_f^0 of PA12 was taken as 95kJ/mol and that of PP was taken as 209 J/g. Figure 9.16 shows that the percentage crystallinity of PA12 and PP is found to be ca. 62% and 50%, respectively and remains almost same on blending. In short, the melting and crystallisation behaviour of uncompatibilised blends reveal that blending has no significant effect on these properties owing to the lack of specific interactions between the components indicating the highly immiscible nature of the blends.

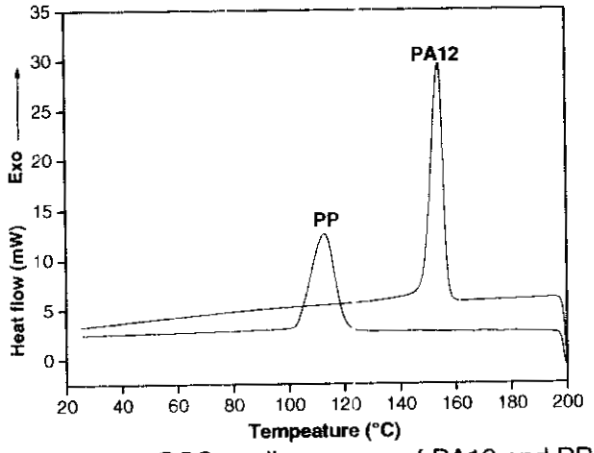

Figure 9.12: DSC cooling curves of PA12 and PP

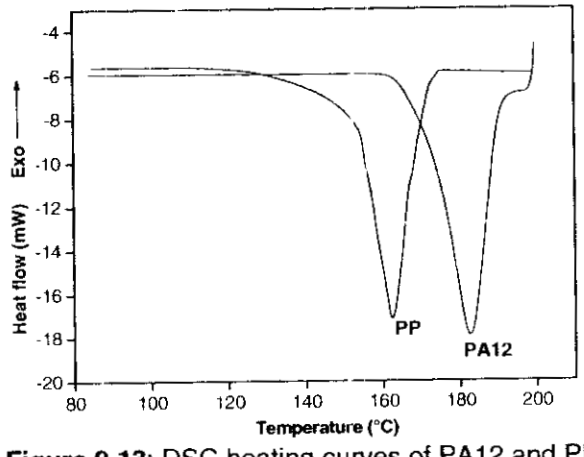

Figure 9.13: DSC heating curves of PA12 and PP

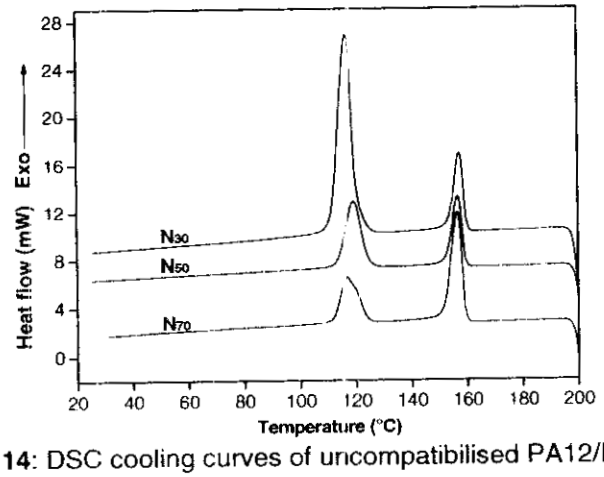

Figure 9.14: DSC cooling curves of uncompatibilised PA12/PP blends

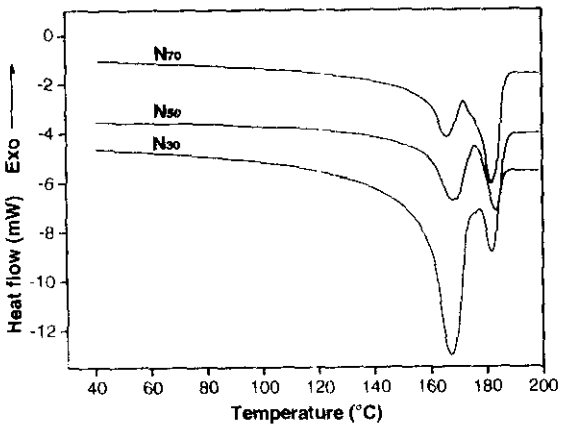

Figure 9.15: DSC heating curves of uncompatibilised PA12/PP blends

Blends	$T_{c,on}$(°C)		T_c(°C)		$T_{m,on}$(°C)		T_m(°C)	
	PA12	PP	PA12	PP	PA12	PP	PA12	PP
N_{100}	157	---	154		175	---	182	---
N_{70}	157	122	154	119	174	157	181	165
N_{50}	157	123	153	117	174	157	180	165
N_{30}	157	122	154	117	175	156	180	166
N_0	---	123	---	117	---	158	---	165

Table 9.13: Effect of blend ratio on the crystallisation and melting temperatures of PA12 and PP

Blends	Normalised			
	ΔH_c (J/g)		ΔH_f (J/g)	
	PA12	PP	PA12	PP
N_{100}	58	---	59	---
N_{70}	61.9	100.3	60.4	101.7
N_{50}	61.6	99.1	58	101.4
N_{30}	59.2	101.6	57.3	103.6
N_0	---	101.1	---	101.3

Table 9.14: Effect of blend ratio on the normalised enthalpies of crystallisation and fusion of PA12 and PP.

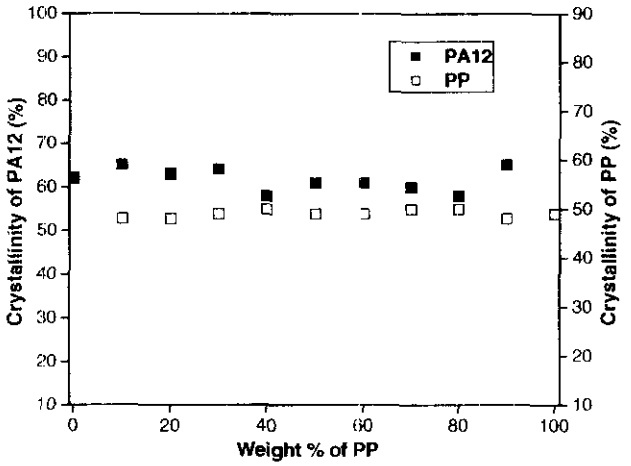

Figure 9.16: Effect of blend ratio on the percentage crystallinity of PA12/PP blends

9.2.2.2. Compatibilised blends

The effect of compatibilisation on the melting and crystallisation properties of N_{70} blends can be evaluated from the cooling and heating curves given in Figs. 9.17 and 9.18, respectively. Table 9.15 shows the T_c and T_m of compatibilised N_{70} blends. It is seen that compatibilisation has no notable effect on the T_c and T_m of the individual polymers. Similarly it can be seen from Table 9.16 that there is no change in the normalised ΔH_c and ΔH_f of PA12 and PP with the addition of compatibiliser.

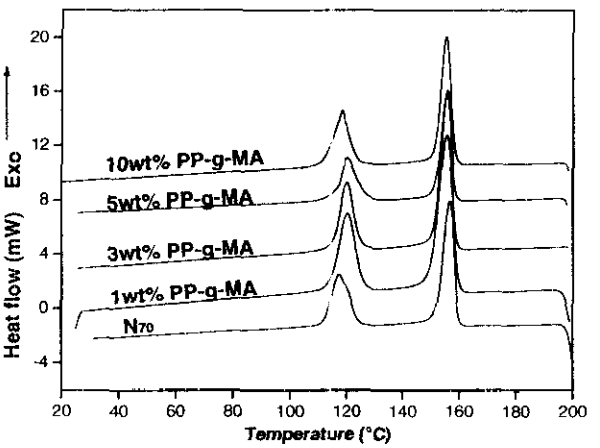

Figure 9.17: Effect of compatibilisation on the cooling curves of N_{70} blends

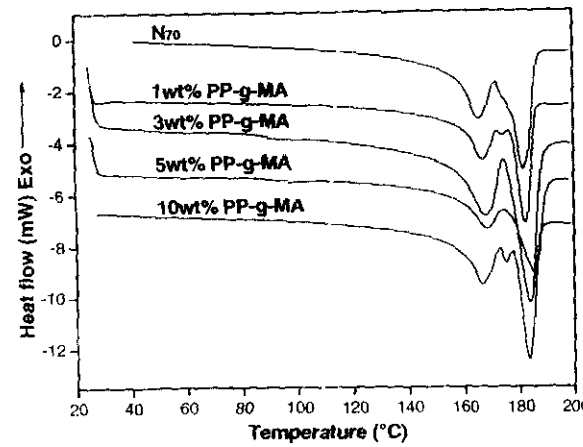

Figure 9.18: Effect of compatibilisation on the heating curves of N_{70} blends

Blends	$T_{c,on}$(°C)		T_c(°C)		$T_{m,on}$(°C)		T_m(°C)	
	PA12	PP	PA12	PP	PA12	PP	PA12	PP
N_{70}	157	122	154	119	174	157	181	165
1wt% PP-g-MA	156	123	153	120	175	157	182	166
3wt% PP-g-MA	156	122	153	120	174	158	183	166
5wt% PP-g-MA	155	123	152	119	174	157	182	165
10wt%PP-g-MA	155	123	152	118	173	156	181	166
15wt%PP-g-MA	156	122	153	119	174	157	181	165

Table 9.15: Effect of compatibilisation on the crystallisation and melting temperatures of PA12 and PP in N_{70} blends

Blends	Normalised			
	ΔH_c (J/g)		ΔH_f (J/g)	
	PA12	PP	PA12	PP
N_{70}	61.9	100.3	60.4	101.7
1wt% PP-g-MA	61.1	99.7	60.3	99.5
3wt% PP-g-MA	60.6	99.2	60.2	98.7
5wt% PP-g-MA	59.2	88.4	59.2	98.2
10wt%PP-g-MA	58.7	98.6	58.7	98.5
15wt%PP-g-MA	58.9	100.3	58.8	98.7

Table 9.16: Effect of compatibilisation on the enthalpies of crystallisation and fusion of PA12 and PP in N_{70} blends

In the case of compatibilised N_{50} blends (Figs. 9.19 and 9.20 as well as Tables 9.17 and 9.18), one can see that compatibilisation has little effect on the melting and crystallisation behaviour of the blends. On the other hand, a different behaviour is exhibited by N_{30} blends. The DSC cooling and heating curves of compatibilised N_{30} blends are given in Figs. 9.21 and 9.22, respectively. The melting and crystallisation behaviour of these blends are evaluated and presented in Tables 9.19 and 9.20. Table 9.19 shows that addition of compatibiliser has no considerable effect on the T_c and T_m of PA12 and PP.

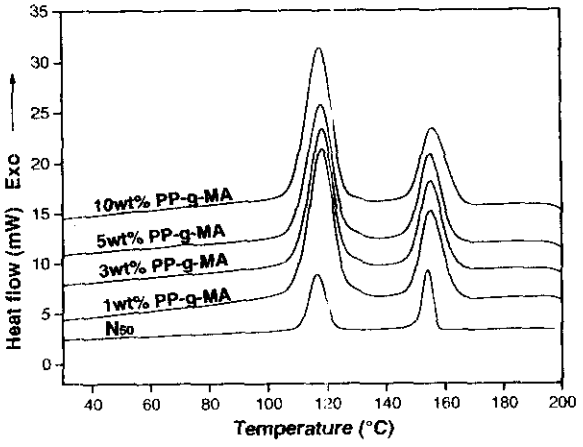

Figure 9.19: Effect of compatibilisation on the cooling curves of N_{50} blends

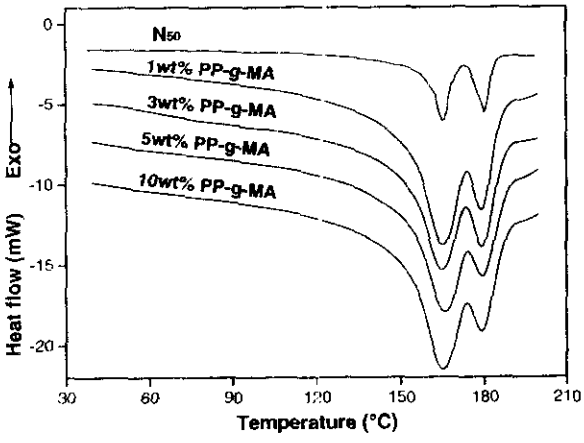

Figure 9.20: Effect of compatibilisation on the heating curves of N_{50} blends

Blends	$T_{c,on}$(°C)		T_c(°C)		$T_{m,on}$(°C)		T_m(°C)	
	PA12	PP	PA12	PP	PA12	PP	PA12	PP
N_{50}	157	123	153	117	174	157	180	165
1wt% PP-g-MA	156	124	152	119	174	157	180	166
3wt% PP-g-MA	155	123	152	119	174	156	179	166
5wt% PP-g-MA	156	124	152	119	174	157	180	165
10wt%PP-g-MA	156	123	153	119	174	156	179	164
15wt%PP-g-MA	157	122	154	119	173	156	179	165
20wt% PP-g-MA	157	124	154	119	174	157	179	166

Table 9.17: Effect of compatibilisation on the crystallisation and melting temperatures of PA12 and PP in N_{50} blends

Blends	Normalised			
	ΔH_c (J/g)		ΔH_f (J/g)	
	PA12	PP	PA12	PP
N_{50}	61.6	99.1	58.2	101.4
1wt% PP-g-MA	61.8	103.4	57.3	103.5
3wt% PP-g-MA	63.4	104.3	55.5	101.5
5wt% PP-g-MA	65.2	106.2	59.2	102.3
10wt%PP-g-MA	62.6	106.1	57.8	105.2
15wt%PP-g-MA	61.6	103.5	58.8	100.2

Table 9.18: Effect of compatibilisation on the enthalpies of crystallisation and fusion of PA12 and PP in N_{50} blends

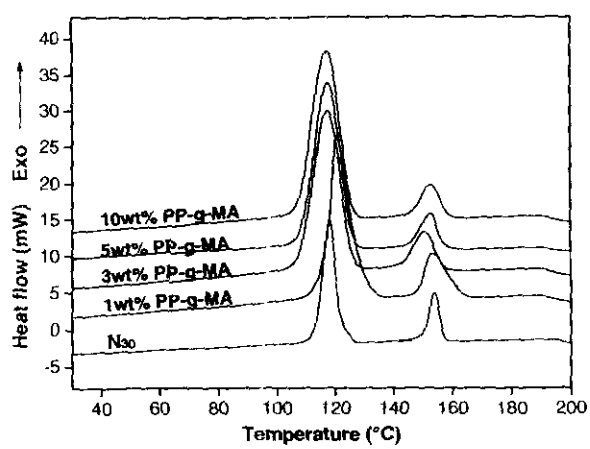

Figure 9.21: Effect of compatibilisation on the cooling curves of N_{30} blends

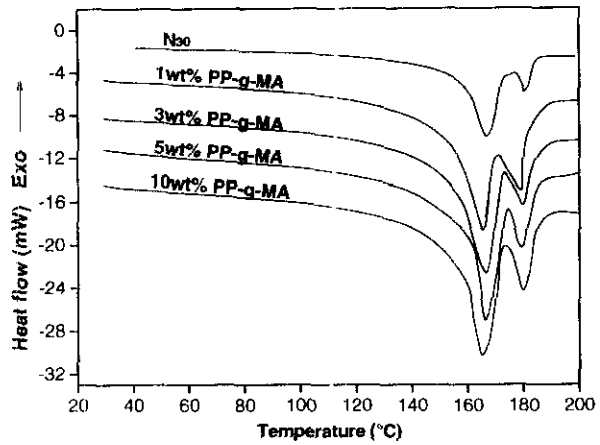

Figure 9.22: Effect of compatibilisation on the heating curves of N_{30} blends

The ΔH_c and ΔH_f values of PA12 and PP in N_{30} blendes given in Table 9.20 offer apparent conflict with the other results. Interestingly, the ΔH_c and ΔH_f of PA12 are considerably affected by the addition of compatibiliser. On the other hand, the ΔH_c and ΔH_f of PP are unaffected. At the same time, there is little change in the T_c and T_m of PA12. Figure 9.23 shows that despite the percentage crystallinity of PA12 is unaffected by compatibilisation in N_{70} and N_{50} blends, there is dramatic decrease in N_{30} blends. On the other hand, compatibilisation has no effect on the percentage crystallinity of PP in all the blends (Fig. 9.24). Why the percentage crystallinity of PA12 decreases with the addition of compatibiliser in N_{30} blends?

Usually, when there are specific interactions between the components in a multiphase system, the crystallisation process of the individual phases will be affected. Based on this fact, one can argue that in N_{30} blends, compatibilisation induces molecular level miscibility between PA12 and PP phases and thereby affects the crystallisation behaviour. However, this can be ruled out due to at least two reasons: (i) compatibilisation of N_{70} and N_{50} blends showed that there is no change in the melting and crystallisation behaviour of PA12 and PP and (ii) the melting and crystallisation behaviour of PP in N_{30} blends is unaffected by compatibilisation.

It should be noted that compatibiliser generally stays at the interface and acts as emulsifying agent rather than to provide molecular level miscibility. At the same time, it is believed that the interfacial chemical reactions occur at the amorphous

regions of polymers. So the change in crystallisation behaviour of compatibilised blends is not solely due to compatibilising action of PP-g-MA. A plausible explanation follows: In N_{30} blends, PP forms the matrix and PA12 phase is dispersed as domains. Note that PP-g-MA is miscible with the matrix and the MA groups of PP-g-MA are projected towards the interfacial region for interfacial chemical reactions with amine end groups of PA12 which are now surrounded by MA groups. During processing at high temperature, some of the MA groups react with amine groups of PA12 to form graft copolymers which act as emulsifying agents. This happens in the melt. However, some of the PP-g-MA molecules which are not involved in the chemical reactions remain as such due to the non-availability of amine groups since PA phase is the minor phase. However, there are possibilities that these PP-g-MA diffuse from the PP phase through the interface towards the PA phase due to the bulk flow. The driving force for this phenomenon is the possibility of chemical reactions. During annealing, PA phase solidifies first in the molten matrix phase of PP. The solidification of PA will restrict the diffusion of the PP-g-MA molecules, which are also in molten state. Thus these molecules will be trapped at the interspherulite region of PA. In DSC measurements, when the polymer crystallises from the melt, the trapped PP-g-MA molecules remain at the interspherulite region. This will deform the PA spherulites and there by decreases the rate of growth of spherulites, consequently the energy liberated during the process decreases.

Blends	$T_{c,on}$(°C)		T_c(°C)		$T_{m,on}$(°C)		T_m(°C)	
	PA12	PP	PA12	PP	PA12	PP	PA12	PP
N_{30}	157	122	154	117	175	156	180	166
1wt% PP-g-MA	156	124	152	120	173	157	180	166
3wt% PP-g-MA	155	123	151	119	173	156	180	167
5wt% PP-g-MA	156	123	153	119	172	155	179	166
10wt%PP-g-MA	155	123	153	119	173	156	179	165
15wt%PP-g-MA	156	123	152	119	173	156	179	165
20wt% PP-g-MA	156	123	152	119	173	155	179	166

Table 9.19: Effect of compatibilisation on the melting and crystallisation behaviour of PA12 and PP in N_{30} blends

Blends	Normalised			
	ΔH_c (J/g)		ΔH_f (J/g)	
	PA12	PP	PA12	PP
N_{30}	59.2	101.6	57.3	103.6
1wt% PP-g-MA	52.1	101.9	52.3	103.3
3wt% PP-g-MA	47.6	104.4	47.5	100.3
5wt% PP-g-MA	45.2	106.3	46.2	102.2
10wt%PP-g-MA	44.3	107.9	45.3	101.5
15wt%PP-g-MA	43.2	107.3	45.1	100.5
20wt% PP-g-MA	42.2	106.2	44.3	101.1

Table 9.20: Effect of compatibilisation on the enthalpies of crystallisation and fusion of PA12 and PP in N_{30} blends

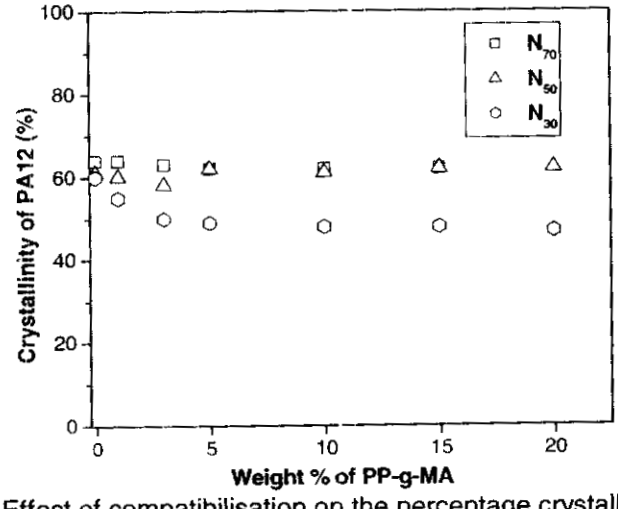

Figure 9.23: Effect of compatibilisation on the percentage crystallinity of PA12 in PA12/PP blends

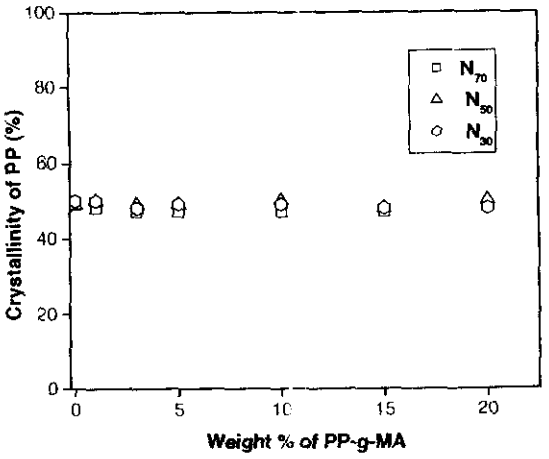

Figure 9.24: Effect of compatibilisation on the percentage crystallinity of PP in PA12/PP blends

9.3. Conclusion

This chapter dealt with the investigation of the effects of blend ratio and compatibilisation on the thermal and crystallisation behaviour of PA12/PP blends. Thermogravimetric studies revealed that blend ratio has significant impact on the thermal stability of the polymers. PA12 was thermally more stable than PP. Addition of 30wt% PP into PA12 didn't alter the thermal stability of the blends. On the other hand, addition of 30wt% PA12 into PP improved the thermal stability of the blends. Phase morphology was found to be one of the decisive factors that affected the thermal stability since the thermal stability depends on the stability of the matrix phase.

Compatibilisation has extensive impact on the thermal stability of the blends. In compatibilised blends also, the rate of improvement of the property depended on the type of morphology. In the present case, maximum improvement in thermal stability was shown by PA12/PP 70/30 blends (since in this case more stable PA12 forms the matrix) followed by 50/50 blends (in which both PA12 and PP are continuous). PA12/PP 30/70 blends showed minimum improvement in thermal stability as in this case PP was the matrix. Further, the merging of degradation peaks was observed for PA12/PP 70/30 blends. In PA12/PP 50/50 blends, despite the peaks approached each other, the degradation peaks of PA12 spitted into two at higher concentration of compatibiliser. For PA12/PP 30/70 blends also, the

degradation peaks approach each other with the addition of compatibiliser, but to a lesser extent and no merging of peaks occurred.

The melting and crystallisation behaviour of the blends revealed that blending has no significant effect on the melting and crystallisation properties of PA12 and PP. Crystallisation temperatures of PA12 and PP were found to be approximately 153 and 117°C, respectively whereas the melting points were approximately 180 and 165°C, respectively. These parameters remained almost the same on blending. Similarly blending didn't affect the enthalpies of crystallisation and fusion PA12 and PP. The percentage crystallinity of the polymers was observed as 60 and 50%, respectively and blending has little effect on the percentage crystallinity of the component polymers due to the highly immiscible and incompatible nature of the blends.

Compatibilisation of 70/30 and 50/50 PA12/PP blends didn't affect the crystallisation and melting behaviour of PA12 and PP. On the other hand, the enthalpies of crystallisation and fusion and consequently, the percentage crystallinity of PA12 in PA12/PP 30/70 blends were decreased remarkably with increase in compatibiliser concentration. This was due to the suppression of growth of spherulites of PA12 during crystallisation process by the diffused PP-g-MA molecules which were trapped at the interspherulite region during processing.

9.4. References

1. I.G. Williams, Plast. Today, **19**, 14, 1984.

2. S.L. Madorsky, Thermal Degradation of Organic Polymers, John Wiley, New York, (1964).

3. C. David in Comprehensive Chemical Kinetics: Degradation of Polymers, vol.14, Ed., C.H. Bawford, C.F.H. Tipper Elsevier, Amsterdam, (1975).

4. A.L. Bhuiyan, Polymer, **25**, 1699, 1984.

5. S.V. Levchik, E.D. Weil, M. Lewin, Polym. Int., **48**, 532, 1999.

6. K.T. Varughese, Kaust. Gum. Kunst., **41**, 114, 1988.

7. A.T. Koshy, B. Kuriakose, S. Thomas, S. Varghese, Polymer, **34**, 2438, 1993.

8. N. Grassie, Ed. Developments in Polymer Degradation, London, Applied Science, (1998).

9. Z. Oommen, G. Groeninckx, S. Thomas, J. Polym Sci. B: Polym. Phys., **38**, 525, 2000.

10. H. Varghese, S.S. Bhagavan, S. Thomas, J. Therm. Anal. Calor., **63**, 749, 2001.

11. H. Varghese, T. Johnson, S.S. Bhagavan, S. Joseph, S. Thomas, G. Groeninckx. J. Polym. Sci. B: Polym. Phys., **40**, 1556, 2002.

12. S. Stack, O. O'Donogbue, C Birkinshaw, Polym. Degrad. Stab., **79**, 29, 2003.

13. N.S. Vrandečić, I. Klarić, T. Kovačić, Polym. Degrad. Stab., **84**, 23, 2004.

14. J. Roeder, R.U.B. Oliveira, D. Becker, M.W. Goncalves, V. Soldi, A.T.N. Pires, Polym. Degrad. Stab., **90**, 481, 2006.

15. K. Aouachria, N.B. Bensemra, Polym. Degrad. Stab., **91**, 504, 2006.

16. P. Malik, M. Castro, C. Carrot, Polym. Degrad. Stab., **91**, 634, 2006.

17. S.P. Vijayalakshmi, G. Madras, J. Appl. Polym. Sci., **101**, 233, 2006.

18. R.N. Santra, P.G. Mukundo, T.K. Chaki, and G.B. Nando, Thermochim. Acta, **219**, 283, 1993.

19. P.P. Lizymol, S. Thomas, Polym. Degrad. Stab., **41**, 59, 1993.

20. R. Ashaletha, M.G. Kumaran, S. Thomas, **61**, 431, 1998.

21. S. George, K.T. Varughese, S. Thomas, Polymer, **41**, 5485, 2000.

22. Z. Oommen, G. Groeninckx, S. Thomas, J. Polym. Sci. B: Polym. Phy., **38**, 525, 2000.

23. J. George, Ph.D Thesis, Mahatma Gandhi University, 2004.

24. S. Joseph, Ph.D Thesis, Mahatma Gandhi University, 2005.

25. E. Martuscelli, C. Silvestre, C. Gismondi, Makromol. Chem., **186**, 2161, 1985.

26. D. Lohse, J. Polym. Eng. Sci., **26**, 1500, 1986.

27. T. Hashimoto, N. Inaba, K. Sato, S. Suzuki, Macromolecules, **19**, 1690, 1986.

28. T. Hashimoto, N.Inaba, N. Yamada, T.S. Suzuki, Macromolecules, **21**, 407, 1988.

29. H. Ito, T.P. Russell, G.D. Wignall, Macromolecules, **20**, 2213, 1987.

30. W.R. Burghardt, Macromolecules, **22**, 2482, 1989.

31. L. D'Orazio, C. Mancarella, E. Martuscelli, G. Sticotti, J. Mater. Sci., **26**, 4033, 1991.

32. L. D'Orazio, C. Mancarella, E. Martuscelli, G. Sticotti, P. Massari, Polymer, **34**, 3671, 1993.

33. L. D'Orazio, C. Mancarella, E. Martuscelli, G. Sticotti, R. Ghisellini, J. Appl. Polym. Sci., **53**, 387, 1994.

34. S. Nojima, K. Sato, T. Ashida, Macromolecules, **24**, 942, 1991.

35. H. Tomura, H. Sato, T. Inoue, Macromolecules, **25**, 1611, 1992.

36. P.M. Cham, T.H. Lee, H. Marand, Macromolecules, **27**, 4263, 1994.

37. H.L. Chen, Macromolecules, **28**, 2845, 1995.

38. C.Y Chen, W. Yunus, H.W. Chiu, T. Kyu, Polymer, **38**, 4433, 1997.

39. S.W. Lim, K.H. Lee, C.H. Lee, Polymer **40**, 2837, 1999.

40. A. Ramanujam, K.J. Kim, T. Kyu, Polymer, **41**, 5375, 2000.

41. J.K. Lee, J.H. Lee, K.H. Lee, B.S. Jin, J. Appl. Polym. Sci., **81**, 695, 2001.

42. G.S. Jang, W.J. Cho, C.S. Ha, J. Polym. Sci. B: Polym. Phys. **39**, 1001, 2001.

43. H. Wang, K. Shimizu, H. Kim, E.K. Hobbie, Z.G. Wang, C.C. Han, J. Chem. Phys., **116**, 7311, 2002.

44. A.M. Rocco, R.P. Bielschowsky, Pereira, Polymer, **44**, 361, 2003.

45. G. Dutt, K.M. Kit, J. Appl. Polym. Sci., **87**, 1984, 2003.

46. N. Dangseeyn, P. Supaphol, M. Nithitanakul, Polym. Test., **23**, 187, 2004.